1. Ahmed Jamal Abdullah Al-Gburi

Center for Telecommunication Research & Innovation (CeTRI), Faculty of Electronics and Computer Technology and Engineering, Universiti Teknikal Malaysia Melaka (UTeM), Jalan Hang Tuah Jaya, Durian Tunggal, Melaka 76100, Malaysia (1)
ORCID: 0000-0002-5305-3937

doi:10.15199/48.2024.04.32

5G MIMO Antenna: Compact Design at 28/38 GHz with Metamaterial and SAR Analysis for Mobile Phones

Abstract. *Meeting the challenge of preserving the compact form of 5G smartphones while accommodating millimeter-wave (mm-wave) bands with a substantial frequency difference, we have introduced an ultra-compact 4-port dual-band multiple-input, multiple-output (MIMO) antenna. This innovative design utilizes a metamaterial-inspired electromagnetic bandgap (EBG) structure to minimize mutual coupling (MC) effectively across a wide frequency range. Constructed on a Rogers TMM4 substrate, the antenna has overall dimensions of 17.76 x 17.76 mm². It incorporates four planar patch antennas placed at the corners, arranged perpendicularly. Each antenna element is optimized for dual-band operation at 28/38 GHz, featuring a rectangular patch with four slots and a full ground plane. The gap between patches measures 0.5 λo, and the EBG ensures efficient and cost-effective reduction of mutual coupling among the MIMO antenna elements. Specific absorption rate (SAR) analysis validates the suitability of this MIMO antenna for 5G mobile phones operating within the targeted frequency band.*

Streszczenie. *Spełniając wyzwanie polegające na zachowaniu kompaktowej formy smartfonów 5G, jednocześnie obsługując pasma fal milimetrowych (fale mm) ze znaczną różnicą częstotliwości, wprowadziliśmy ultrakompaktowy 4-portowy, dwuzakresowy, wielokanałowy, wielowejściowy i wielowyjściowy (MIMO)) antena. Ta innowacyjna konstrukcja wykorzystuje inspirowaną metamateriałem strukturę elektromagnetycznego pasma wzbronionego (EBG), aby skutecznie minimalizować wzajemne sprzężenie (MC) w szerokim zakresie częstotliwości. Antena, zbudowana na podłożu Rogers TMM4, ma wymiary całkowite 17,76 x 17,76 mm². Zawiera cztery płaskie anteny krosowe umieszczone w rogach, ułożone prostopadle. Każdy element anteny jest zoptymalizowany do pracy dwuzakresowej w paśmie 28/38 GHz, z prostokątną łatką z czterema szczelinami i pełną płaszczyzną uziemienia. Szczelina między polami wynosi 0,5 λo, a EBG zapewnia wydajną i opłacalną redukcję wzajemnego sprzężenia pomiędzy elementami anteny MIMO. Analiza współczynnika absorpcji specyficznej (SAR) potwierdza przydatność tej anteny MIMO do telefonów komórkowych 5G działających w docelowym paśmie częstotliwości.* (***Antena 5G MIMO: kompaktowa konstrukcja przy 28/38 GHz z metamateriałami i analizą SAR dla telefonów komórkowych***)

Keywords: Electromagnetic bandgap (EBG), Millimeter-Wave, Four-port, multiple-input multiple-output (MIMO), 5G, Mobile Phones,
Słowa kluczowe: Pasmo wzbronione elektromagnetyczne (EBG), fala milimetrowa, cztery porty, wiele wejść i wiele wyjść (MIMO

Introduction

The rapid evolution of 5G technology brings improvements in wireless communication network performance, such as reduced latency, enhanced data throughput, better connectivity, and increased spectral efficiency [1-3]. MIMO antenna technology plays a crucial role in 5G devices, positively impacting channel capacity across various systems [4], [5]. Millimeter-wave communications offer advantages like extensive bandwidth, expanded spectrum resources, and compact antenna dimensions [6], [7]. The FCC has allocated frequencies in the 28 GHz, 37 GHz, 39 GHz, and 64 - 71 GHz range for 5G use [8].

Addressing signal attenuation challenges in these bands, antenna experts design high-gain, broad-spectrum antennas to combat path loss and atmospheric absorption [9–13]. The proliferation of antenna elements enhances system capacity, signal quality, and reduces multipath interference [14–16].

Maintaining separation between MIMO elements is a challenge impacting mutual coupling within the desired frequency range [17], [18]. Implementing a MIMO approach with robust isolation improves overall system performance, offering higher data rates, increased capacity, reduced multipath interference, and improved reliability [19–21].

Recent research highlights dual-frequency MIMO antennas operating at 28/38 GHz, showcasing various designs with high isolation and peak gains [2, 7, 10, 15, 22, 23]. This study builds on a single-element design [24], adapting dimensions and shape to create a 4-port orthogonal MIMO antenna with a Dielectric Resonator (DR) method for mutual coupling reduction.

The proposed antenna supports 5G millimeter-wave frequencies at 28/38 GHz, featuring four dual-band channels. Utilizing the EBG technique for high isolation, the antenna is cost-effective, constructed on a Rogers TMM4 substrate (17.76 × 17.76 mm²). Importantly, it allows for a significant increase in the number of antenna elements while effectively reducing mutual coupling.

Four-Port MIMO Antenna Design with SAR Analysis

This section addresses the configuration of a 4-port MIMO antenna and explores the methods employed to enhance isolation among its components. To achieve high isolation between ports, we present EBG reduction technique. The dimensions of every four-port MIMO array design that has been proposed are 17.76 mm ×17.76 mm × 1.52 mm. Fig. 1(a) illustrates the arrangement of four identical single antenna units, each positioned 5mm apart from the others, oriented orthogonally to one another. The Rogers TMM4 substrate, is the foundation for the proposed antenna array. The optimum MIMO dimensions is listing as follow: X = Y = 17.76 mm, and g_x=g_y=5 mm. CST Microwave Studio 2019 is used to simulate the antenna array. In Fig. 1(b), you can see the representation of the equivalent resonance circuit model for the four orthogonal elements of the MIMO system. Each element is individually excited through a separate 50 Ω terminal. It's important to note that there is always some degree of coupling between nearby antennas. This coupling, which occurs between the adjacent antennas, is mathematically modeled using LC series lumped elements. You can find the specific values for each component in Table 1. The return loss of the proposed MIMO antenna resonates at two main frequencies, which are 28 GHz and 38 GHz as shown in Fig.1(c). Fig. 2 illustrates the mutual coupling across ports in a quad-port MIMO array without the use of any isolation techniques. In this depiction, you can observe insufficient isolation within the desired frequency band.

Metamaterial-Inspired EBG for the Design of a 4-Port MIMO with Low MC

Enhancing the MIMO parameters is a primary objective in the development of 5G millimeter-wave wireless terminals. To achieve this, the utilization of an EBG structure is proposed as a means to bolster these attributes.

Additionally, the square shape employed in this design as an EBG enhances the mutual interaction between antenna elements and MIMO parameters. EBGs are designed to substitute dielectric lenses for gain improvement by providing an effect of high refractive index. The MIMO antenna along with EBG cells are presented in Figs. 3(a), 3(b) and 3(c).

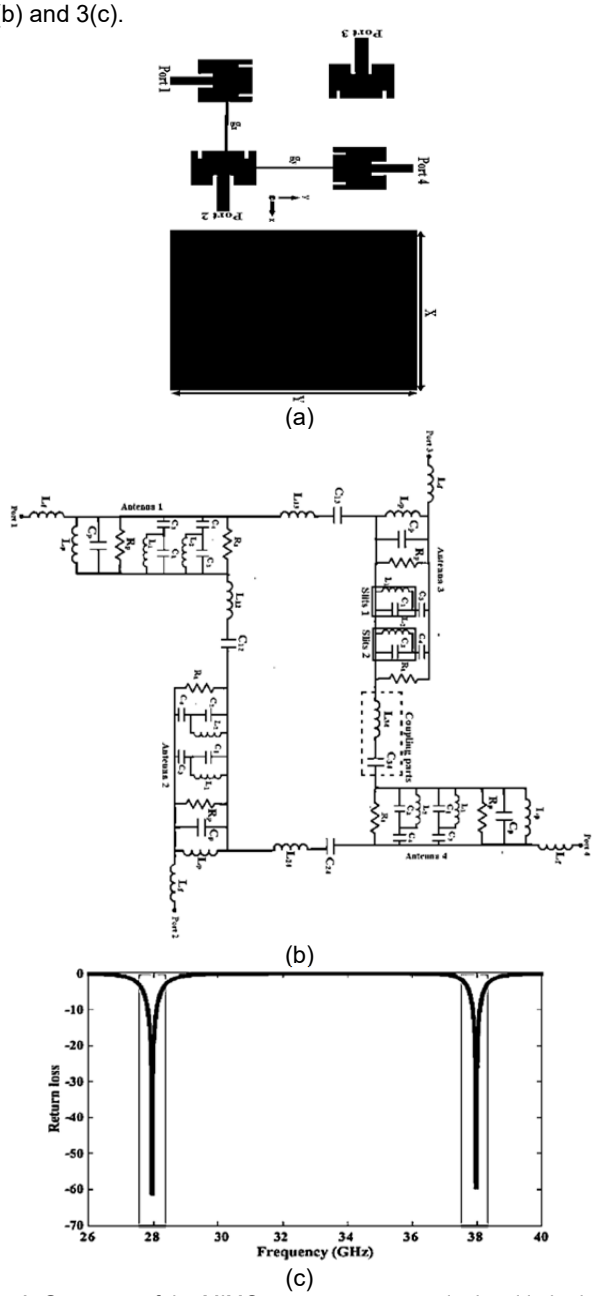

Fig.1. Geometry of the MIMO antenna array, as depicted in both its (a) top and bottom views, and (b) equivalent circuit and (c) return loss.

Table 1. Summarizes the equivalent circuit variables for the suggested MIMO antenna array.

L_f	L_p	C_p
9.4 pH	10.6 pH	3.85 pF
L_{12}	C_{12}	L_{13}
9.2 pH	4 pF	8.9 pH
R_p	C_1	L_1
50 Ω	0.2 PF	9.4 pH
C_{13}	L_{34}	C_{34}
3.6 pF	8.7 pH	6.75 pF
C_2	L_3	C_3
8.4 pF	10.4 pH	2 pF
L_{24}	C_{24}	C_4
10 pH	4 pF	0.6 pF
R_1	50 Ω	

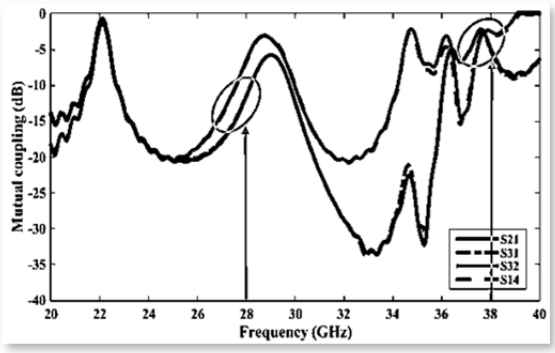

Fig. 2. Displays the simulated mutual coupling between the ports in the absence of any decoupling techniques.

Table 2 lists the planned EBG unit cell's measurements. The substrate is made of Rogers TMM4 material, which has a typical thickness of 1.52 mm (ε = 4.5). As an initial estimation for the EBG sheet that should be inserted between the MIMO antenna elements, the suggested EBG unit cell is analyzed. This investigation involves using CST with EBG periodic boundary conditions to simulate multiple cells, as depicted in Fig.3 (c). In Fig. 3 (d), the equivalent circuit of the EBG unit cells is depicted. In this context, C_{e1} corresponds to the capacitance arising from the presence of an air gap between adjacent EBG unit cells. C_{e2}, on the other hand, represents the capacitance resulting from the dielectric gap situated between the top metallic patch and the ground plane. The symbol 'L' represents the inductance of the metallic vias, which is contingent on the radius denoted as 'r.' When working with an EBG structure characterized by specific parameters, including 1) substrate thickness (h), 2) patch width `ascertain the magnitudes of the inductor (L) and capacitors (C_1 and C_2) by utilizing the formulas:

$$(1)\quad C_{e1} = \frac{\varepsilon_0 W_p}{\pi} arch\left(\frac{g+W_p}{g}\right)$$

$$(2)\quad C_{e2} = \frac{\varepsilon_0 \varepsilon_r W\cdot}{\pi} arch\left(\frac{\sinh(\pi(W\cdot+g)/4h)}{\sinh(\frac{\pi g}{4h})}\right)$$

$$(3)\quad L = \mu_0 h\left\{\frac{1}{\pi}\left[\ln\left(\frac{a+\sqrt{a^2+2r^2}}{2r}\right) + \ln 2^{0.5}\right]\right\}$$

$$(4)\quad F_0 = \frac{1}{2\pi\sqrt{LC}}$$

Here, $W\cdot = 1 - 2S/W_p^2 W_p$, $S = \pi r^2$, $a = W + g$, $C = C_{e1} + C_{e2}$, and S S denotes the area of the cross-section of the via hole, with μ_0, ε_0 representing the vacuum's permeability and permittivity, respectively. Fig. 3 (e) displays the methodology steps of applying EBG technique.

Table 2. Variables for the suggested MIMO antenna with EBG geometry (all dimensions in mm).

variables	Value
X	17.76
Y	17.76
W_1	1.4
W_2	4.4
W_3	7.4
W_4	0.4
g_1	0.1
g_2	0.1

The properties, including permeability, refractive index, and effective permittivity, are shown in Fig.4. According to Fig.4, the permittivity at the two resonance frequencies of 28 GHz and 38 GHz is less than unity. The antenna's gain can therefore be increased by printing the array of unit cells. The Rogers TMM4 substrate, which has a 4.5 dielectric constant, is the foundation for the proposed antenna array.

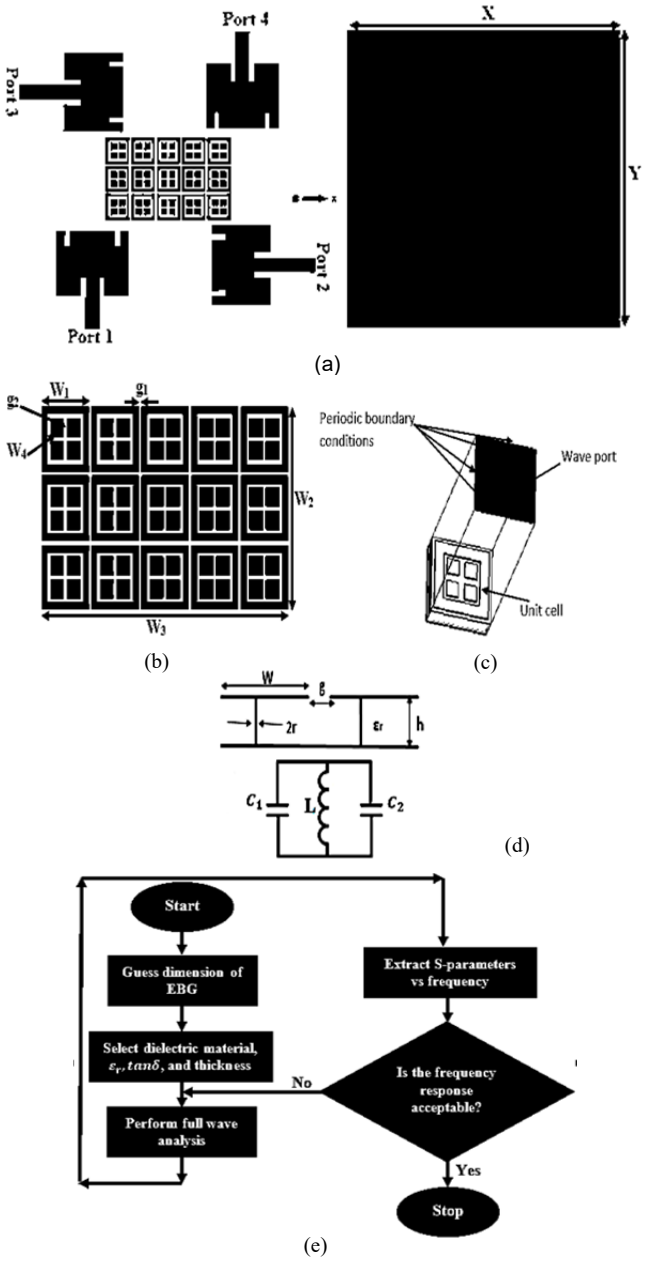

Fig.3. A quad-port MIMO antenna representation with EBG. (a) Top view, (b) EBG sheet, (c) EBG unit cell simulation condition, (d) Equivalent circuit of EBG, and (e) flow chart of applying EBG technique.

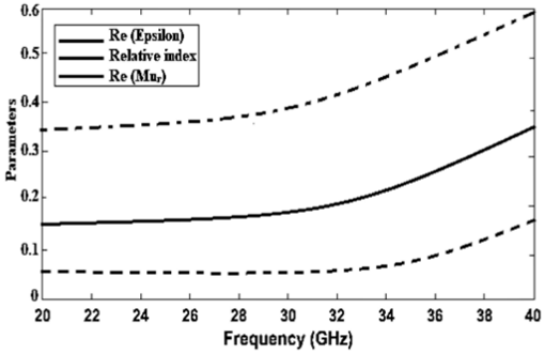

Fig.4. The properties of the suggested EBG unit cell, including refractive index (n), as well as permittivity and permeability.

Radiation Characteristics and Influence of User Hand and Head

The assessment of electromagnetic (EM) energy absorbed by the human body during mobile phone usage is expressed through a metric referred to as Specific Absorption Rate (SAR). Given that the suggested MIMO antenna structure is affixed to the back cover, it's essential to predict its Specific Absorption Rate (SAR) value. This back cover is made from a dielectric material with a permittivity of 3.32 and a loss tangent of 0.002. Fig.5 (a) illustrates the antenna's configuration with the back cover, which has dimensions of 150×70×1.2 mm³.

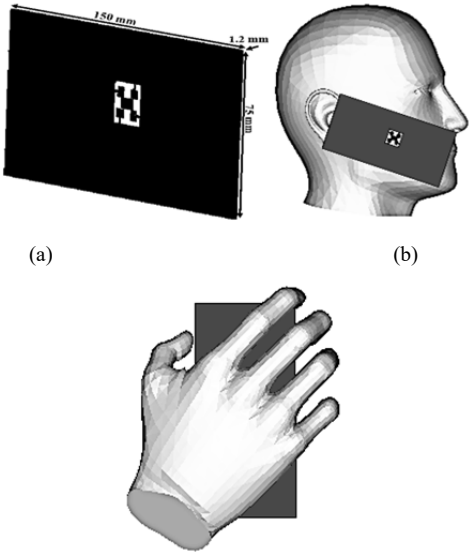

Fig.5. (a) Antenna schematic with a dielectric back cover, (b) the configuration of the antenna arrangement involving a hand phantom model, and (c) the design for SAR analysis utilizing a head phantom model.

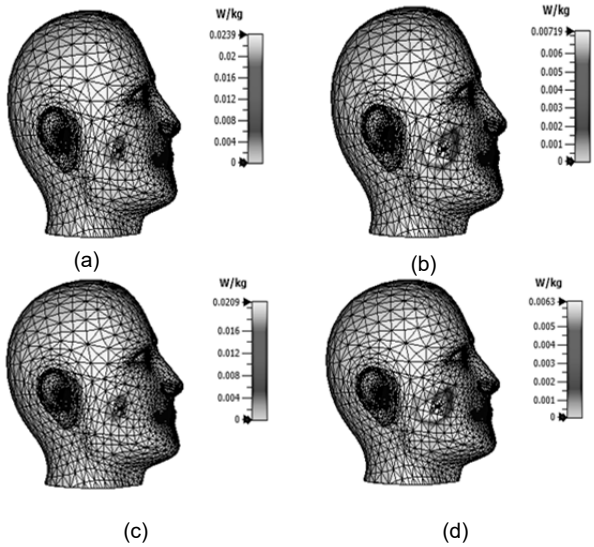

Fig.6. Displays the simulated SAR at 15 dBm for the proposed MIMO antenna configuration with a back cover, focusing on 28 GHz. It provides SAR results for (a) 1 g and (b) 10 g, and also includes data at 38 GHz, featuring (c) 1 g and (d) 10 g.

Given that the envisaged antenna is intended for mobile handsets, it is crucial to anticipate its SAR. As shown in Fig. 5(b), the arrangement layout is designed to assess the electromagnetic energy absorbed by the human head using a human head phantom model. The antenna is situated at an angle of 650 degrees with reference to the negative vertical axis. It's worth noting that the SAR value is significantly influenced by the separation distance between the antenna element and different parts of the human body. In our study, the simulation positions the MIMO antenna 5 mm away from the head phantom model, specifically near the ear and mouth regions of the head phantom model.

In Fig.5 (c), the setup arrangement of the MIMO antenna is displayed over a Single Hand Mode model (SHM), designed to evaluate its performance in data mode. The orientation and positioning of the antenna are optimized to align with the most comfortable user scenarios. Notably, there exists a minimal gap of approximately 0.2 mm between the ground plane of the MIMO antenna and the hand phantom model.

Fig.6 illustrates the simulated SAR value, and it is noteworthy that the calculated SAR falls within the acceptable range of standard SAR values (1.6 W/Kg). The impact of the user's hand on the MIMO antenna is assessed for both resonance frequencies of 28 GHz and 38 GHz. Importantly, the position of the antenna over the hand significantly affects the antenna's performance

Conclusions

In this study, we introduced a quad-port MIMO array distinguished by robust port isolation. Our approach involved implementing the Electromagnetic Band Gap (EBG) technique to mitigate mutual coupling between antennas, and we thoroughly evaluated its effectiveness. Using CST STUDIO SUITE version 2019, we conducted simulations to optimize the dimensions of the radiating elements. The suggested MIMO antenna was specifically designed to operate at two resonance frequencies, which are 28/38 GHz. The EBG technique played a crucial role in enhancing the isolation between antennas, primarily due to the introduction of additional capacitance in the circuit. The results obtained from these analyses consistently exhibited positive trends within the two operational frequency bands. This suggests that our recommended antenna structure holds promise for utilization in 5G millimeter-wave and mobile phones.

Acknowledgements

The authors gratefully acknowledge Universiti Teknikal Malaysia Melaka (UTeM) and the Ministry of Higher Education (MOHE) in Malaysia for their support in this research.

The correspondence address is: *Ahmed Jamal Abdullah Al-Gburi, Center for Telecommunication Research & Innovation (CeTRI), Faculty of Electronics and Computer Technology and Engineering, Universiti Teknikal Malaysia Melaka (UTeM), Jalan Hang Tuah Jaya, Durian Tunggal, Melaka 76100, Malaysia; email: ahmedjamal@ieee.org*

REFERENCES

[1] Nizar S., Anouar B., Islem B. H., Lassaad L., and Ali G., "Millimeter-Wave Dual-Band MIMO Antennas for 5G Wireless Applications", Journal of Infrared, Millimeter, and Terahertz Waves, vol. 44, pp. 297–312, 2023. https://doi.org/10.1007/s10762-023-00914-5

[2] Ayyaz Ali, Mehr E Munir, Moustafa M. Nasralla, Maged A. Esmail, Ahmed Jamal Abdullah Al-Gburi, Farooq Ahmed Bhatti, Design process of a compact Tri-Band MIMO antenna with wideband characteristics for sub-6 GHz, Ku-band, and Millimeter-Wave applications, *Ain Shams Engineering Journal*, 2023, 102579.

[3] Elabd, R.H., Al-Gburi, A.J.A. Super-Compact 28/38 GHz 4-Port MIMO Antenna Using Metamaterial-Inspired EBG Structure with SAR Analysis for 5G Cellular Devices. J Infrared Milli Terahz Waves (2023). https://doi.org/10.1007/s10762-023-00959-6.

[4] R. K. Mistri et al., "Quad Element MIMO Antenna for C, X, Ku, and Ka-Band Applications," *Sensors*, vol. 23, no. 20, p. 8563, Oct. 2023, doi: 10.3390/s23208563.

[5] Elabd RH, Al-Gburi AJA. SAR assessment of miniaturized wideband MIMO antenna structure for millimeter wave 5G smartphones. *Microelectron En* 2023;112098

[6] Parchin N. O., Basherlou H. J., Al-Yasi Y.I. A., Abdulkhaleq A.M., Patwary M. and Abd-Alhameed R.A., " A New CPW-Fed Diversity Antenna for MIMO 5G ", Electronics, vol. 9, pp. 261-276, 2020. doi:10.3390/electronics9020261

[7] C. R. Jetti et al., "Design and Analysis of Modified U-Shaped Four Element MIMO Antenna for Dual-Band 5G Millimeter Wave Applications," *Micromachines*, vol. 14, no. 8, p. 1545, Jul. 2023, doi: 10.3390/mi14081545.

[8] Khan J., Ullah S., Ali U., Tahir F. A., Peter I., and Matekovits L., "Design of a millimeter-wave mimo antenna array for 5G communication terminals", Sensors, vol. 22, no. 7, 2022. https://doi.org/10.3390/s22072768.

[9] Shayea I., Tharek A. R., Marwan H. A., and Rafiqul I., "Real measurement study for rain rate and rain attenuation conducted over 26 GHz microwave 5G link system in Malaysia" , IEEE Access, vol.6, pp. 19044–19064, 2018.

[10] Ali W., Sudipta D., Hicham M., and Soufian L., "Planar dual-band 27/39 GHz millimeter- wave MIMO antenna for 5G applications", Microsystem Technologies, vol. 27, pp. 283-292, 2021.

[11] Zahra H., Wahaj A. A., Wael A. E. A., Niamat H., Syed M. A., and Subhas M., "A 28 GHz Broadband Helical Inspired End-Fire Antenna and Its MIMO Configuration for 5G Pattern Diversity Applications", Electronics, vol.10, no. 4, pp.405-419, 2021.

[12] Hussain N., Wahaj A. A., Wael A., Syeda I. Na, Abir Z., and Tuan T. L., "Compact wideband patch antenna and its MIMO configuration for 28 GHz applications." AEU International Journal of Electronics and Communications, vol. 132, pp. 153612, 2021.

[13] Ibrahim A. A., and Wael A. A., "High gain, wideband and low mutual coupling AMC-based millimeter wave MIMO antenna for 5G NR networks", AEU-International Journal of Electronics and Communications, vol. 142, pp. 153990, 2021.

[14] Jilani S. F., and Akram A., "Millimetre-wave T-shaped MIMO antenna with defected ground structures for 5G cellular networks." IET Microwaves, Antennas & Propagation, vol.12, no. 5, pp. 672–677, 2018.

[15] A. Ali et al., "A Compact MIMO Multiband Antenna for 5G/WLAN/WIFI-6 Devices," *Micromachines*, vol. 14, no. 6, p. 1153, May 2023, doi: 10.3390/mi14061153.

[16] Hala M. M., Mohamed I. A. and Abdelhamed A. S. , "A Novel Dual-band 28/38 GHz Slotted Microstrip MIMO Antenna for 5G Mobile Applications", Journal of Electromagnetic Waves and Applications, vol. 33, pp. 1581–1590, 2019.

[17] A. Khabba et al., "A new miniaturized wideband self-isolated two-port MIMO antenna for 5G millimeter-wave applications", *TELKOMNIKA Telecommunication Computing Electronics and Control*, vol. 21, no. 3, pp. 630-630, Feb. 2023.

[18] T. Saeidi, A. J. A. Al-Gburi, and S. Karamzadeh, "A Miniaturized Full-Ground Dual-Band MIMO Spiral Button Wearable Antenna for 5G and Sub-6 GHz Communications," *Sensors*, vol. 23, no. 4, p. 1997, Feb. 2023, doi: 10.3390/s23041997.

[19] Yang B., Zhiqiang Y., JiLan R. Z., Jianyi Z., and Wei H., "Digital beam forming- based massive MIMO transceiver for 5G millimeter-wave communications", IEEE Transactions on Microwave Theory and Techniques, vol. 66, no. 7, pp. 3403–3418, 2018.

[20] Ohyun J., Jung-Ju K., Jungmin Y., Dooseok C., and Wonbin H., "Exploitation of dual polarization diversity for 5G millimeter-wave MIMO beam forming systems" , IEEE Transactions on Antennas and Propagation, vol. 65, no. 12, 6646-6655, 2017.

[21] Mneesy T. S., Radwa K. H., Amira I. Z., and Wael A. E. A., "A Novel High Gain Monopole Antenna Array for 60 GHz Millimeter-Wave Communications", Applied Sciences, vol. 10, no. 13, pp. 4546, 2020.

[22] Marzouk H. M., Mohamed I. A., and Abdel Hamied S., "Novel dualband 28/38 GHz MIMO antennas for 5G mobile applications", Progress in Electromagnetics Research, vol. 93, pp.103–117, 2019.

[23] Aliakbari H., Abdolali A., Alessandra C., Diego M., Rashid M., and Pedram M., "ANN-based design of a versatile millimetre-wave slotted patch multi-antenna configuration for 5G scenarios", IET Microwaves, Antennas & Propagation, Vol. 11, no. 9, pp. 1288–1295, 2017.

[24] Gómez L., and Ibrahim A.S., "Design, Analysis and Simulation of Microstrip Antenna Arrays with Flexible Substrate in Different Frequency, for Use in UAV-Assisted Marine Communications", J. Mar. Sci. Eng., vol.11, pp. 730, 2023 https://doi.org/10.3390/jmse11040730.